Cretaceous Research 50 (2014) 238–251

Contents lists available at ScienceDirect

Cretaceous Research

journal homepage: www.elsevier.com/locate/CretRes

Maastrichtian carbon cycle changes and planktonic foraminiferal bioevents at Gebel Matulla, west-central Sinai, Egypt

Sherif Farouk*

Exploration Department, Egyptian Petroleum Research Institute, Nasr City 11727, Egypt

ARTICLE INFO

Article history:
Received 3 July 2013
Accepted in revised form 28 February 2014
Available online 29 May 2014

Keywords:
Campanian-Maastrichtian
Planktonic foraminifera
Biostratigraphy
Carbon-isotope stratigraphy
Sudr Formation
Gebel Matulla
Sinai
Egypt

ABSTRACT

Comparison between the planktonic foraminiferal bioevents from different palaeolatitudes suggests that the biostratigraphic criteria used to identify the Maastrichtian stage boundaries are problematic. A new high-resolution calibration of planktonic foraminiferal biostratigraphic, carbon-isotope, and sequence-stratigraphic criteria has been recorded for the first time from the Maastrichtian Sudr Formation at Gebel Matulla, west-central Sinai. The sedimentary successions allow the identification of prominent long-term carbon isotope events in the Maastrichtian, namely the negative excursion of the Campanian–Maastrichtian Boundary Event (CMBE), the positive excursion of the mid-Maastrichtian Event (MME), and the decline towards the Cretaceous-Palaeogene transition (KPgE). Termination of these well known $\delta^{13}C$ events is associated with unconformities, created by eustatic sea-level changes, although the long duration argues for superimposed local tectonic control.

1. Introduction

Marine biotic migration patterns and shifts in foraminiferal $\delta^{18}O$ on a global scale indicate several short-term periods of climatic cooling and warming in the Maastrichtian that occurred superimposed on the long-term Late Cretaceous cooling (e.g. Barrera and Huber 1990, Li and Keller 1998a, Barrera and Savin, 1999, Friedrich et al., 2009, Thibault and Gardin 2010). Prominent high-amplitude sea-level falls, recorded between 78–76, 71–70 and 67–66 Ma from coastal and platform sediments in both hemispheres, argue for a highly variable environmental system globally (Crampton et al., 2006; Simmons et al., 2007).

However, a reliable correlation of climatic events and the sedimentary record of sea-level change is still a matter of debate. Recent advances have been achieved by the application of carbon-isotope stratigraphy, which is emerging as a powerful tool in global correlation. A global Maastrichtian carbon-isotope correlation was developed based on numerous high-resolution $\delta^{13}C$ records from sites in Boreal and Tethyan shelf seas, as well as the open ocean (Thibault et al., 2012a,b; Voigt et al., 2012). This correlation allows for the identification of prominent long-term events in the Maastrichtian, namely the Campanian–Maastrichtian Boundary Event (CMBE), the mid-Maastrichtian Event (MME), and the Cretaceous-Palaeogene transition (KPgE). In addition, some of the $\delta^{13}C$ records show significant superimposed high-frequency variations which are thought to be controlled by orbitally forced climate change (Voigt et al., 2012). The integration of stratigraphic data allows for consideration of the temporal relation between changes in sea level and the global carbon cycle.

The climatic evolution of the Late Cretaceous led to increased bio-provinciality of planktonic microfossil assemblages into distinct Tethyan, Intermediate, Boreal and Austral provinces that persisted to the end of the Maastrichtian (Shafik, 1990; Huber, 1992; Huber and Watkins, 1992; Burnett, 1998; Lees, 2002; Thibault et al., 2012a,b). Many authors noted the absence of key markers or variations in the range of these species at different palaeolatitudes, and this led to several different planktonic foraminiferal and nannofossil zonal schemes.

In northern Egypt, a huge submerged carbonate platform developed, formed by the calcareous hemipelagic facies of the Campanian–Maastrichtian Sudr Formation with its abundant and diverse planktonic microfossil assemblage. In Sinai, the Sudr Formation was deposited in an open marine environment at outer neritic to bathyal depths (300–500 m) as indicated by the benthic foraminifera (see also Luger, 1988; Speijer and Van der Zwaan, 1996). The present study is the first comprehensive investigation of a new $\delta^{13}C$ record of bulk carbonates from southern part of the Tethyan Province calibrated with planktonic foraminiferal

* Tel.: +20 2 01281719573.
E-mail address: geo.sherif@hotmail.com.

http://dx.doi.org/10.1016/j.cretres.2014.02.021

biostratigraphy and sequence stratigraphy of the Maastrichtian Sudr Formation in the Gebel Matulla section. Data collected from this study allows for detailed correlation with the δ13C record from deep ocean successions such as the Tercis les Bains Maastrichtian GSSP and Gubbio sections, and ODP Hole 1210B in the western Pacific (Voigt et al., 2012; Fig. 1).

2. Geological setting

Sinai is located between the African and Arabian plates, separated by the Gulf of Suez and Gulf of Aqaba-Dead Sea rift system (Fig. 2). The sedimentary succession along the eastern side of the Gulf of Suez is subdivided into three main sequences representing the (1) Proterozoic to Eocene pre-rift; (2) Oligocene–Miocene syn-rift; and (3) Quaternary post-rift stages (Fig. 2). The Matulla section is exposed along a range of almost north–south orientated hills which are located 3 km southwest of the city of Abu Zenaima, west-central Sinai (29°01′02″N, 33°12′45″E; Fig. 2). The highest crest point is 421 m above sea level. The sedimentary succession comprises six formations of shallow platform sediments, namely the Matulla (Coniacian–Santonian), Sudr (Maastrichtian), Dakhla (Danian–Selandian), Tarawan (Thanetian), Esna (Thanetian–Ypresian) and Thebes (Ypresian) formations (Figs. 2 and 3).

The Campanian–Maastrichtian Sudr Formation (Ghorab, 1961) is widely distributed in Sinai with an average thickness of about 100–150 m. It unconformably overlies the Coniacian–Santonian 170 m-thick Matulla Formation which consists of a lower sandstone unit and an upper shale unit with intercalated carbonate beds separating the overlying transgressive carbonate facies of the Sudr Formation by a sharp contact that is easily recognized in the field. The Sudr Formation in Egypt starts with the *Globotruncanita elevata* Zone of early Campanian age (Farouk and Faris, 2012). In the present study at Gebel Matulla, the whole Campanian falls within an hiatus in the Matulla section. This discontinuity reflects structural activity of the Gebel Matulla that began in the latest Santonian and ended in the late Campanian (Fig. 4).

The late Santonian tectonic event corresponds to the first general compressional episode registered by the African–Arabian plate during the Alpine Cycle, which resulted in major changes in the topography of North and Central Africa, with the development of narrow fold-induced relief and the uplift of large areas (Guiraud and Bosworth, 1999; Guiraud et al., 2005).

The Sudr Formation comprises an hemipelagic facies of chalky limestone and limestones, and represents a period of elevated rates of carbonate sedimentation across northern Egypt. Deep middle to outer shelf foraminiferal wacke/packstone forms the greater part of the formation. It yields an abundant and diverse fauna of planktonic and benthic foraminifera, indicating a period of transgression, while diagenetically-cemented, calcareous mudstones of the inner shelf with ferruginous coatings and decreased foraminiferal diversity reflect regressive periods. The Sudr Formation is conformably overlain by the Dakhla Formation, which consists of 12 m of grey marls with interbedded shales and is of latest Maastrichtian–Paleocene age in the Matulla section (Fig. 3). The basal part of the Dakhla Formation of latest Maastrichtian age may change laterally into carbonate in other parts of Sinai, marked by a sharp erosive contact between the Sudr and Dakhla formations towards the north.

3. Material and methods

A total of 325 samples were collected from the Sudr Formation at intervals of 20–40 cm. The study interval is marked by a high diversity and abundance of generally well preserved planktonic foraminifera of a Tethyan low-latitude assemblage. For foraminiferal analyses, about 200 g of dry rock sample were soaked in 10% hydrogen peroxide, disaggregated in water, washed through a 63 μm sieve, and then dried. For this qualitative study, all residues were investigated under an Olympus SZX7 binocular microscope at a maximum magnification of x90. A total of 75 planktonic foraminiferal species were identified in Maastrichtian sediments at the Matulla section. The most important foraminifera are illustrated in Figs. 5 and 6 using scanning electron microscopy of the Geological Survey of Egypt.

For stable isotope analyses, bulk-carbonate samples were dried, micro-drilled and weighed. Carbon isotope measurements were performed in the stable isotope laboratory (Goethe-University Frankfurt) by reaction with purified phosphoric acid (H_3PO_4) at a reaction temperature of 72 °C using a Finnigan MAT 253 with Gasbench. All isotope values are reported in ‰ relative to the Vienna Peedee belemnite standard (V-PDB). The analytical

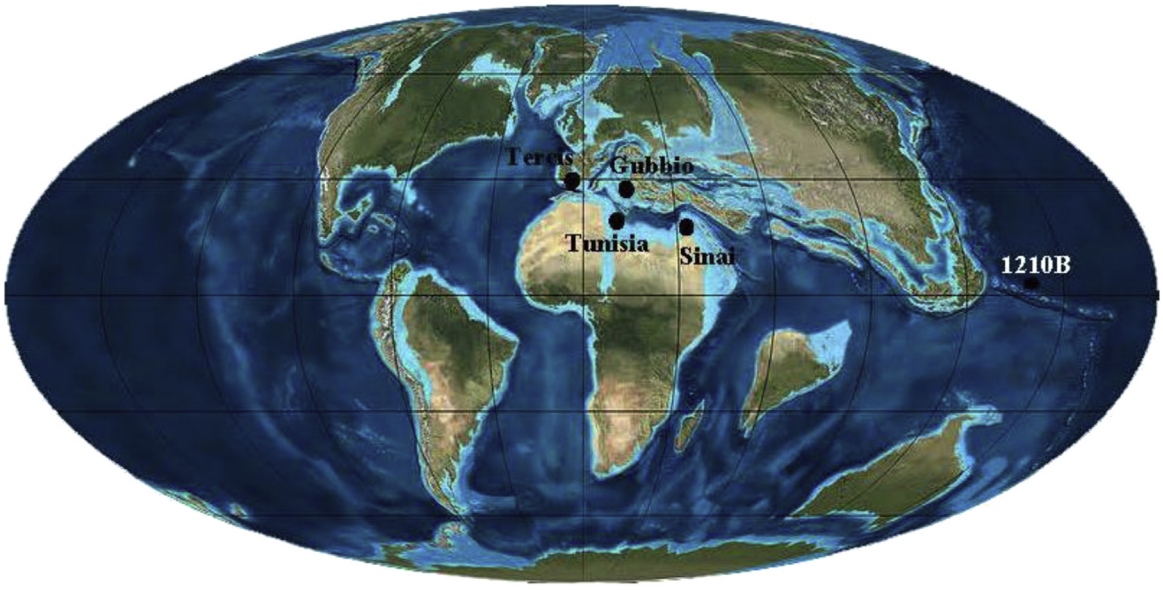

Fig. 1. Palaeogeographic map of the early Maastrichtian (70 Ma) showing position of localities used in this study (after cpgeosystem.com).

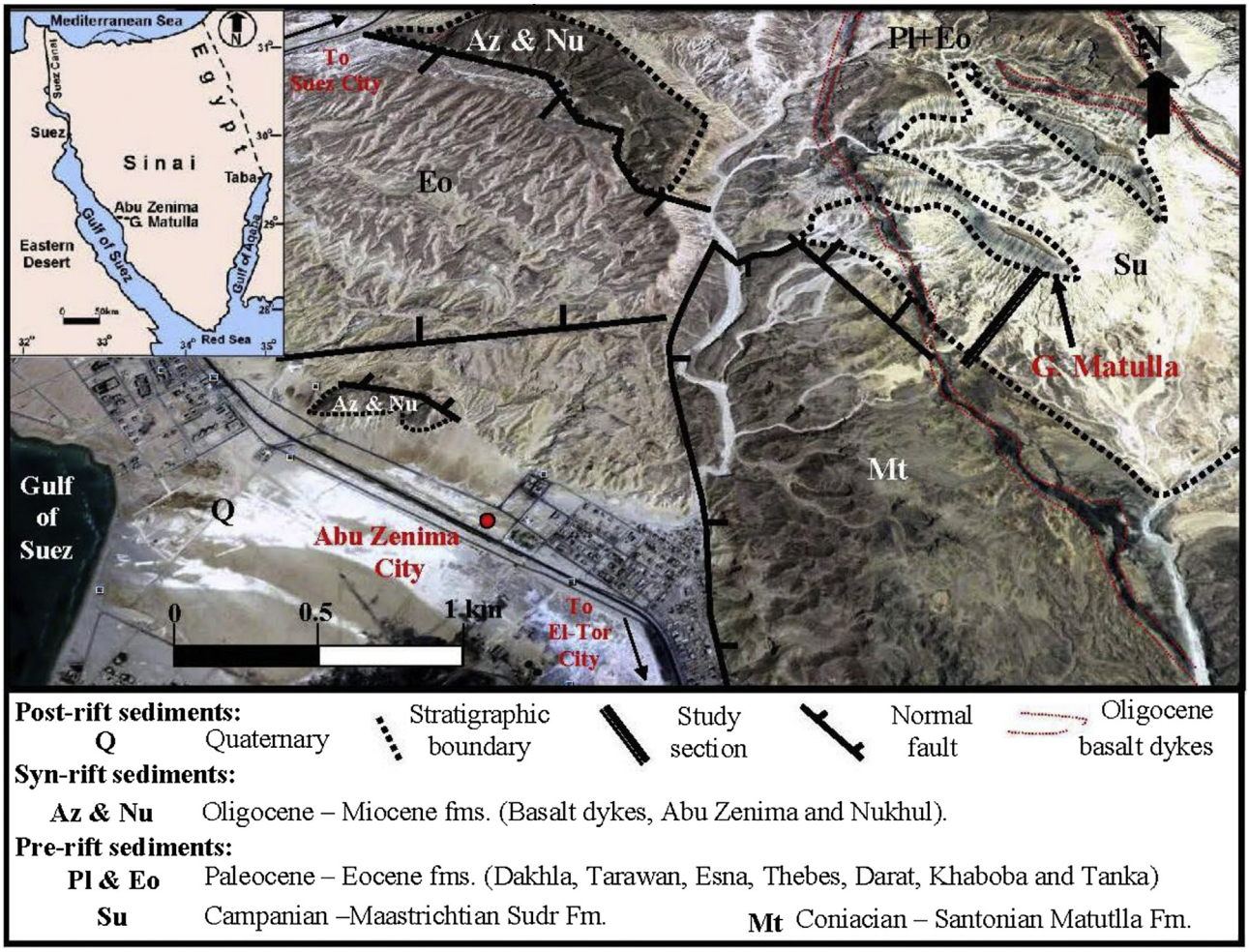

Fig. 2. (A) Schematic map showing the location of the Matulla section in west-central Sinai, Egypt. (B) Interpreted satellite image with faults and the distribution of Cretaceous and Cenozoic lithostratigraphic units.

precision of repeated standard measurements is better than 0.06 and 0.08‰ for carbon and oxygen respectively.

4. Biostratigraphy

The standard zonation and estimated ages of Li et al. (1999) is used with some modification based on the highest and lowest occurrence, (HO, LO) of the marker species. The following planktonic foraminiferal zones can be identified in the Matulla section (Figs. 7, 8 and 9).

4.1. *Rugoglobigerina hexacamerata* Zone (CF8b)

Definition: Interval zone from the LO of *Rugoglobigerina hexacamerata* Brönnimann to the LO of *Gansserina gansseri* (Bolli).
Author: Li et al. (1999).
Estimated age: earliest Maastrichtian (71.0–70.39 Ma; Li et al., 1999).
Thickness: 25.8 m (samples 11 to 85); equivalent to the lowermost part of the Sudr Formation in Gebel Matulla which overlies the upper Santonian Matulla Formation (Fig. 7).
Assemblage: The dominant planktonic foraminiferal species recorded in this zone include *Globotruncana ventricosa* White, *G. arca* (Cushman), *G. aegyptiaca* Nakkady, *G. orientalis* El-Naggar, *G. duwi* (Nakkady), *G. bulloides* Vogler, *G. linneiana* (d'Orbigny), *Globotruncanita stuartiformis* (Dalbiez), *G. stuarti* (de Lapparent), *Contusotruncana fornicata* (Plummer), *Rugoglobigerina rugosa* (Plummer), *R. macrocephala* Brönnimann, *Heterohelix globulosa* (Ehrenberg), *H. navaroensis* Loeblich, *H. reussi* (Cushman) and *H. striata* (Ehrenberg) (Fig. 7).
Remarks: Faris and Abu Shama (2006) defined the late Campanian–early Maastrichtian *Tranolithus phacelosus* CC23 nannofossil Zone at the base of the Sudr Formation in the Matulla section. They also stated that the Campanian–Maastrichtian stage boundary occurs between the subzones CC 23a and CC 23b at the HO of *Aspidolithus parcus constrictus* [i.e. *Broinsonia parca constricta*] without a break in the nannofossil assemblages in the Abu Zenima area. In the present study, the author considers this part is equivalent to the planktonic foraminiferal *Rugoglobigerina hexacamerata* Zone (CF8b) of earliest Maastrichtian age (Figs. 8 and 9). The HOs of *Broinsonia parca constricta* were recorded at the base of Chron C31r in the Tercis les Bains GSSP (France) and Gubbio (Italy) sections and in the Indian Ocean (Gardin et al., 2012; Thibault et al., 2012a,b).

4.2. *Gansserina gansseri* Zone (CF7)

Definition: Interval from the LO of *Gansserina gansseri* to the LO of *Racemiguembelina powelli* (Smith and Pessagno).
Author: Brönnimann (1952)

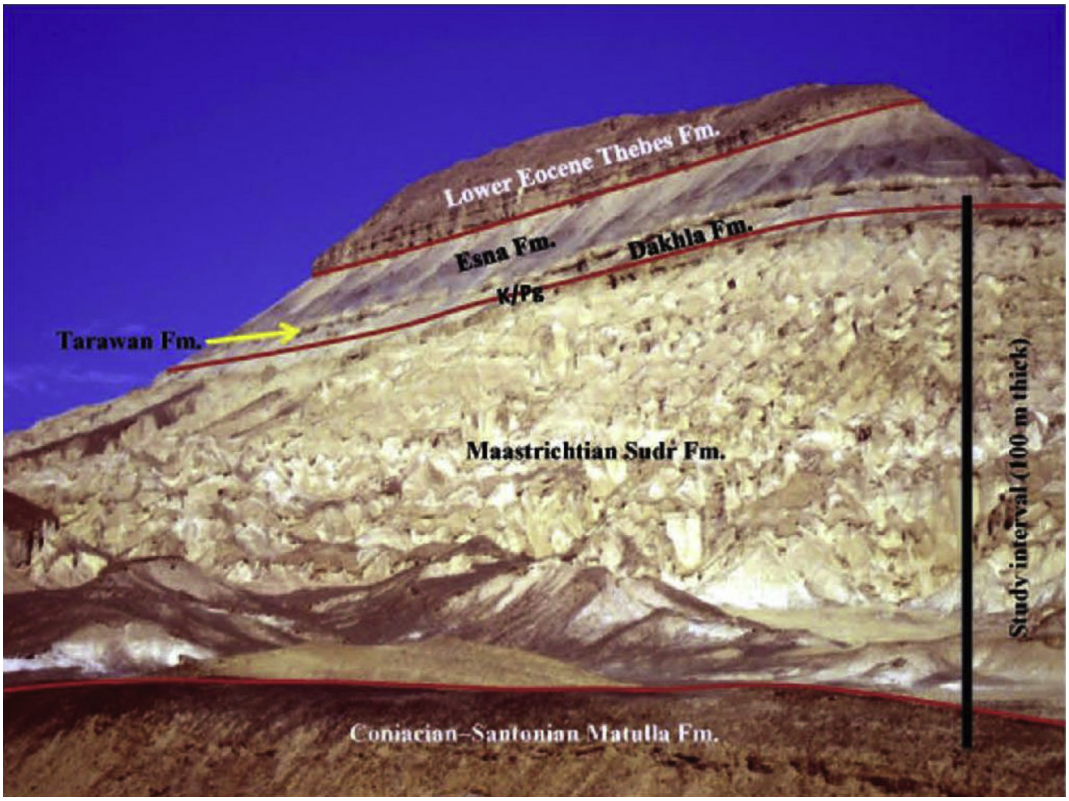

Fig. 3. Outcrop image of the Matulla section with (A) the studied Maastrichtian interval of the Sudr Formation and (B) the K/Pg transition with the uppermost Maastrichtian Sudr Formation, became the Paleocene- early Eocene Dakhla, Tarawan, Esna and Thebes formations; view to north-west.

Fig. 4. Close up showing the tectonic activity across the Matulla/Sudr formational boundary (about 10 km north-east of Gebel Matulla; view to north-east).

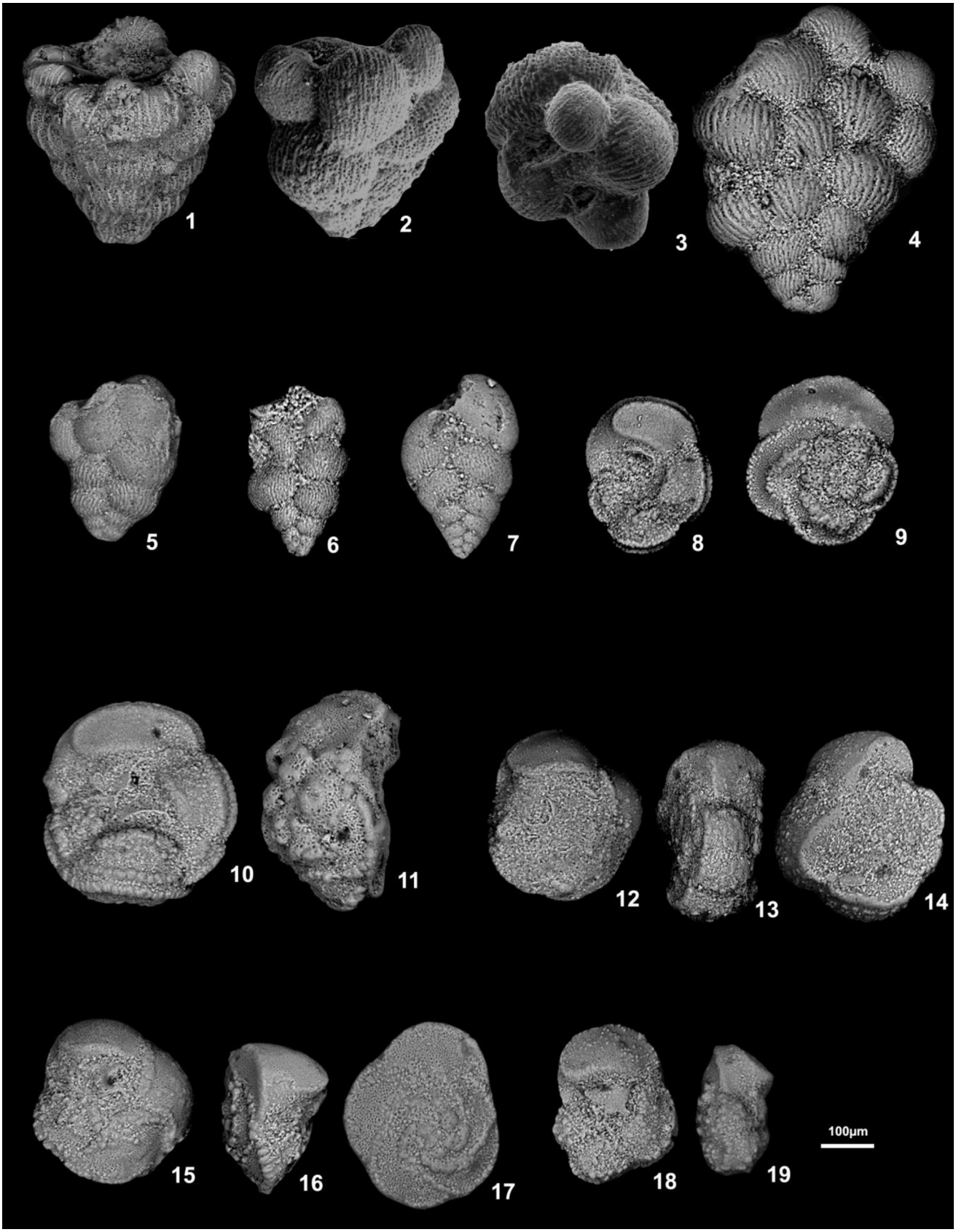

Fig. 5. 1: *Racemiguembelina fructicosa* (Egger), sample no. 298. 2–3: *Racemiguembelina powelli* (Smith and Pessagno), sample no. 165. 4: *Planoglobulina brazoensis* Martin, sample no. 206. 5: *Planoglobulina carseyae* (Plummer), sample no. 206. 6: *Pseudoguembelina hariaensis* Nederbragt, sample no. 289. 7: *Heterohelix labellosa* Nederbragt, sample no. 285. 8–9: *Contusotruncana fornicata* (Plummer), sample no. 13. 10–11: *Contusotruncana plicata* (White), sample no. 180. 12–17: *Gansserina gansseri* (Bolli), sample no 207. 18–19: *Globotruncana aegyptiaca* Nakkady, sample no. 15.

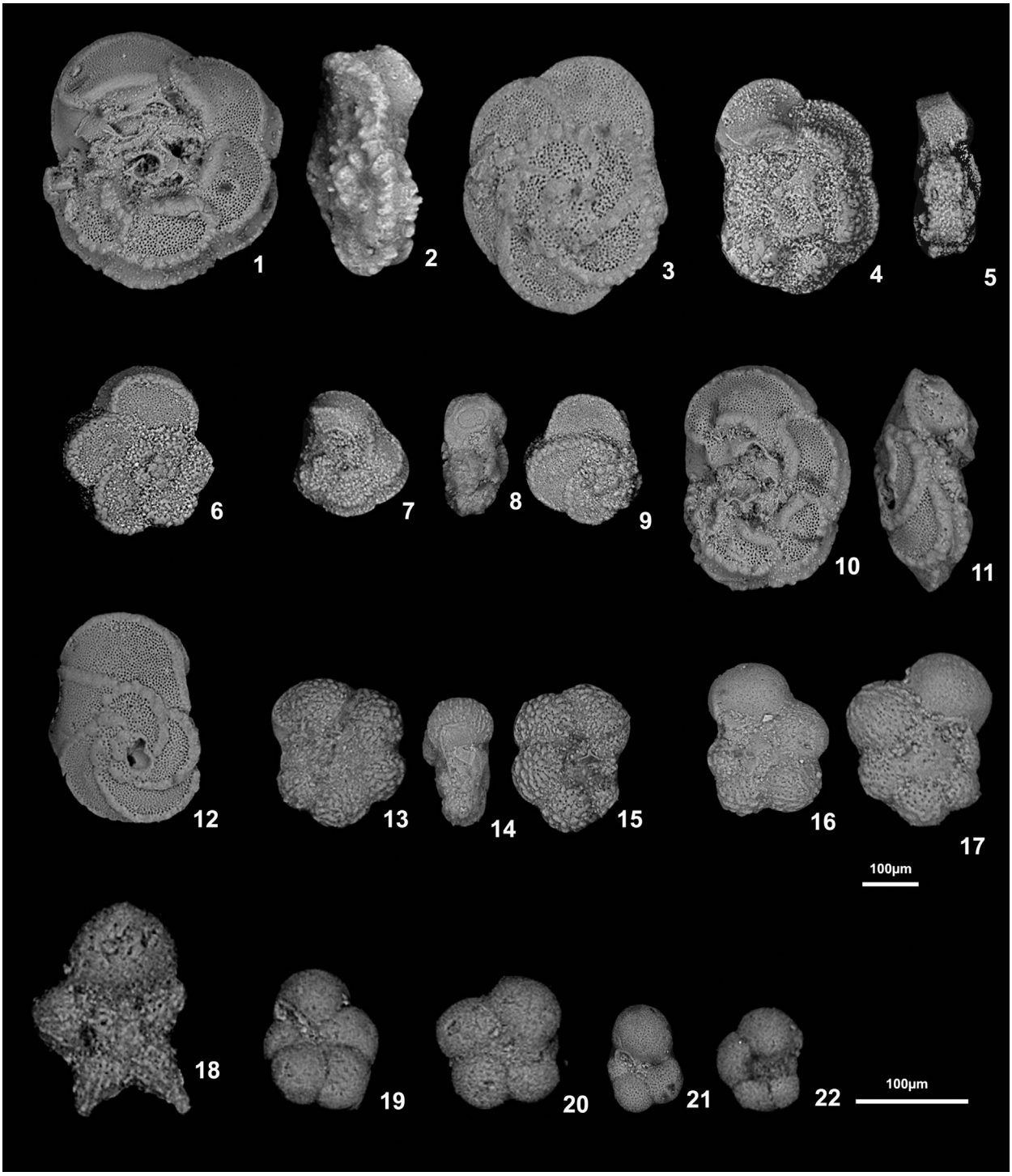

Fig. 6. 1–3: *Globotruncana arca* (Cushman), sample no. 17. 4–6: *Globotruncana linneiana* (d'Orbigny), sample no. 150. 7–9: *Globotruncana bulloides* Vogler, sample no. 30. 10–12: *Globotruncana mariei* Banner and Blow, sample no. 50. 13–15: *Rugoglobigerina hexacamerata* Brönnimann, sample no. 30. 16–17: *Rugoglobigerina scotti* (Brönnimann), sample no. 290. 18: *Plummerita hantkeninoides* (Brönnimann), sample no. 301. 19: *Parvularugoglobigerina eugubina* (Luterbacher & Premoli Silva), sample no. 311. 20: *Eoglobigerina pentagona* (Morozova), sample no. 311. 21: *Eoglobigerina fringa* (Subbotina), sample no. 311. 22: *Eoglobigerina eobulloides* (Morozova), sample no. 311.

Estimated age: early Maastrichtian (70.4–69.6 Ma; Li et al., 1999).
Thickness: 23.1 m (samples 86 to159) in the lower part of the Sudr Formation at Gebel Matulla (Fig. 7).
Assemblage: Foraminifera are abundant with moderate to good preservation. The assemblage of this interval is similar to that of the underlying CF8b Zone, with the addition of the nominate taxon, and *Pseudoguembelina palpebra* Brönnimann and Brown (Fig. 7).

Remarks: Globally the LO of *Gansserina gansseri* is not a reliable bioevent due to variations in the position of the LO of *Gansserina gansseri* at different palaeolatitudes (Fig. 10). In the Tercis les Bains GSSP, Gubbio and Indian Ocean ODP sites 762 and 763, the LO is reported from the uppermost Campanian (e.g. Premoli-Silva and Sliter 1995, Robaszynski and Caron, 1995; Robaszynski et al., 2000; Odin, 2001; Osman, 2003; Gardin et al., 2012). In low-

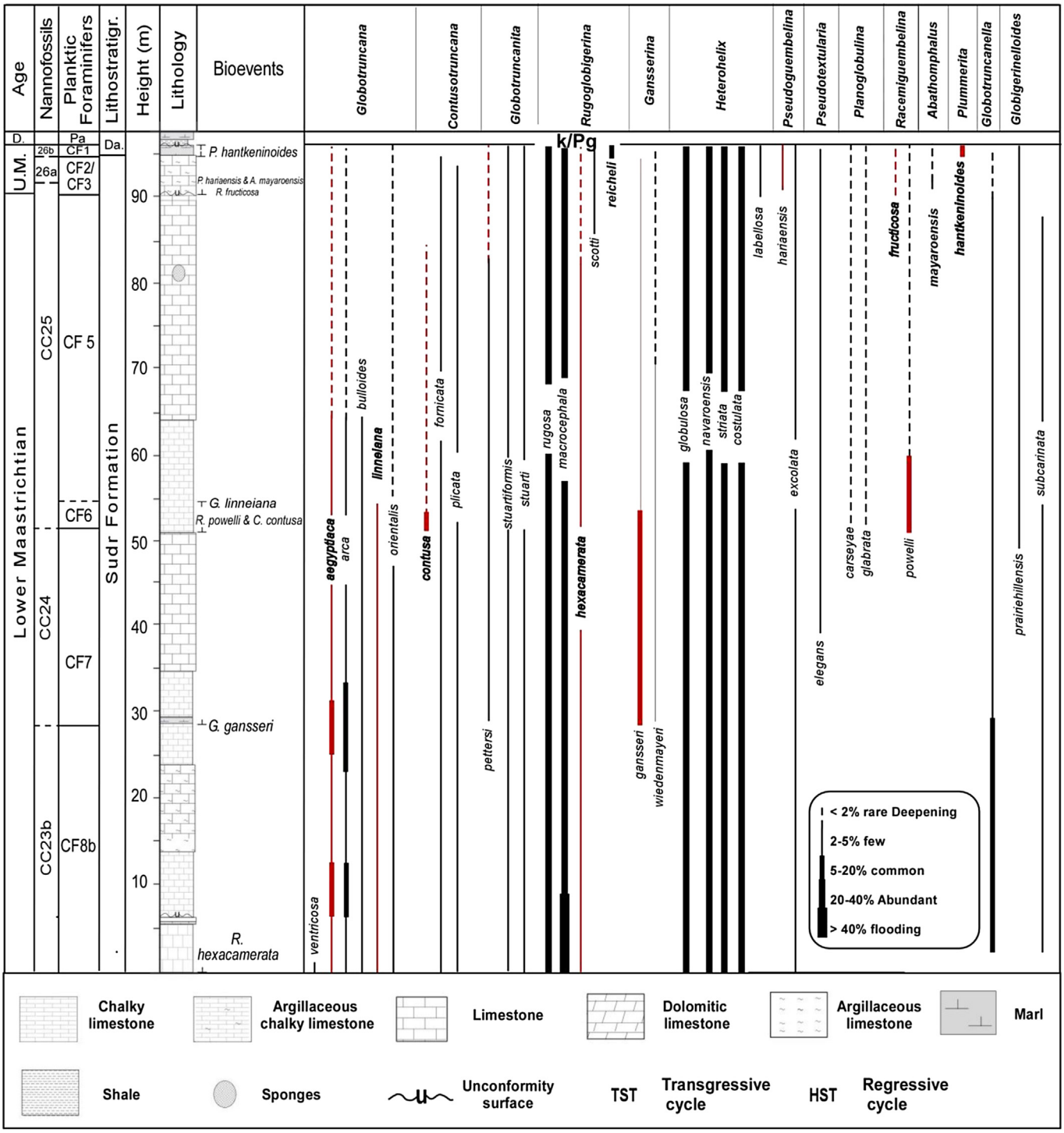

Fig. 7. Lithologic log of the Matulla section, western Sinai, Egypt with the range of planktonic foraminifera. The nannofossil zonation is that of Faris and Abu Shama (2006) and Al-Wosabi and Abu Shama (2007).

latitude successions such as in Tunisia, Jordan and Egypt, this event is relatively high and the index-species is found in the middle part of the lower Maastrichtian, (Abed and Ashour, 1987; Li et al., 1999 and 2000; Samir, 2002; Ayyad et al., 2003; Hewaidy et al., 2006; El-Azabi and Farouk, 2011).

4.3. *Racemiguembelina powelli* Zone (CF6)

Definition: Partial range zone from the LO of *Contusotruncana contusa* to the HO of *Globotruncana linneiana* (d'Orbigny).

Author: Defined herein.

Estimated age: early Maastrichtian (69.6–69.1 Ma; Li et al., 1999).

Thickness: 2.7 m (samples 159 to 169) in the middle part of the Sudr Formation at Gebel Matulla (Fig. 7).

Assemblage: Planktonic foraminifera are frequent and well preserved. The assemblage of this interval is similar to that of the underlying CF5 Zone. In addition to the LO of *Racemiguembelina powelli*, *Contusotruncana contusa* (Cushman), *Planoglobulina carseyae* (Plummer) and *P. glabrata* (Cushman) are recorded from this zone (Fig. 7).

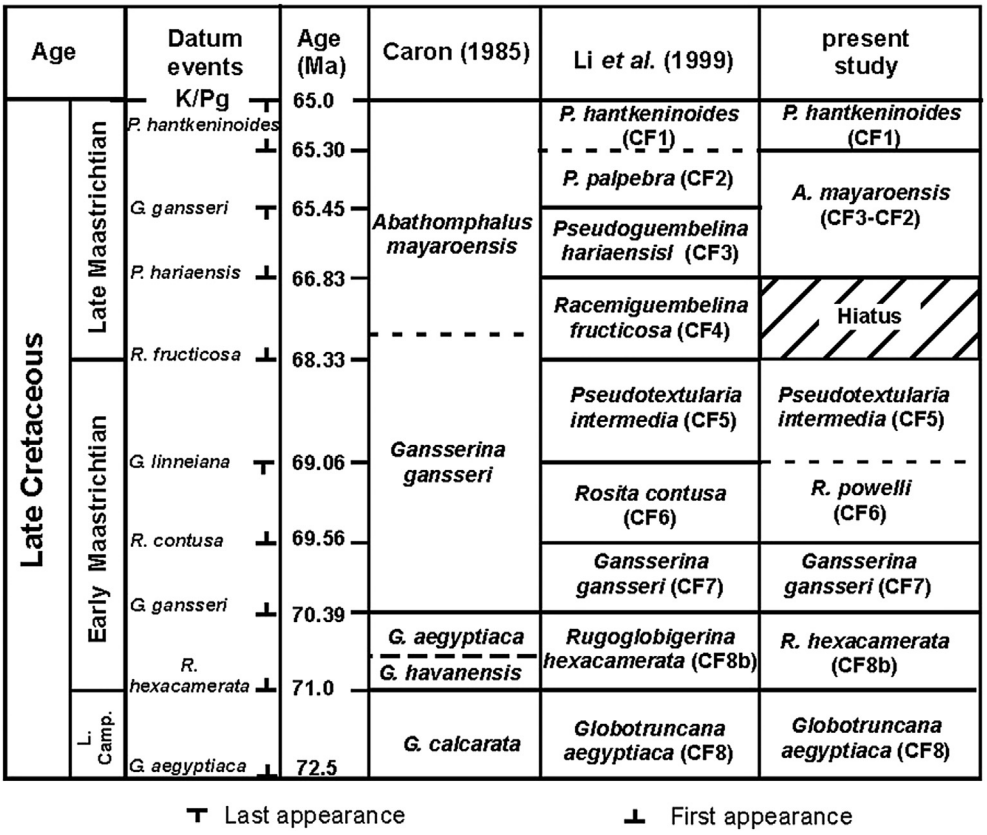

Fig. 8. Scheme of biozonation with planktonic foraminifera using the studies of Caron (1985), Li et al. (1999) and results of this study.

Remarks: This proposed zone is equivalent to the *Contusotruncana contusa* Zone, which was emended by Li and Keller (1998a,b). However, *Contusotruncana contusa* is a rare species and its LO is strongly diachronous. Thus, it is located slightly above the base of the Maastrichtian in the Tercis Les Basins GSSP section (Odin, 2001) but significantly higher in the Gubbio area, in DSDP Hole 525B in the southern Atlantic Ocean (Premoli Silva and Sliter, 1995; Gardin et al., 2012; Fig. 10), in Spain (Pérez-Rodríguez et al., 2012), Tunisia and Egypt (Li et al., 2000; Samir, 2002). Because of these problems in using *Contusotruncana contusa*, the LO of *Racemiguembelina powelli* is used as an alternative bio-event in the present study.

4.4. *Pseudotextularia intermedia Zone (CF5)*

Definition: Partial range zone from the HO of Globotruncana linneiana to the LO of Racemiguembelina fructicosa (Egger).
Author: Introduced by Nederbragt (1990) and modified by Li and Keller (1998).
Estimated age: early Maastrichtian (69.1–68.3 Ma; Li et al., 1999).
Thickness: 35.2 m (samples 170 to 283) in the middle part of the Sudr Formation at Gebel Matulla (Fig. 7).
Assemblage: Planktonic foraminifera are frequent and moderately preserved. The assemblage of this interval is similar to that of the underlying CF4 Zone, except for the absence of *Globotruncana linneiana* (Fig. 7). The LO of *Rugoglobigerina scotti* (Brönnimann) and *Guembelitria cretacea* Cushman occur in the higher parts of this zone (Fig. 7).
Remarks: This zone is approximately equivalent to the upper part of the *Gansserina gansseri* Zone of Caron (1985; Fig. 7).

4.5. Abathomphalus mayaroensis *Zone (*CF3-CF2*)*

Definition: Interval range zone from the LO of *Abathomphalus mayaroensis* to the LO of *Plummerita hantkeninoides* Brönnimann.
Author: The zone was introduced by Nederbragt (1990) and modified by Li and Keller (1998a).
Estimated age: late Maastrichtian (66.8–65.3 Ma; Li et al., 1999).
Thickness: 4.7 m (samples 284 to 297) in the upper part of the Sudr Formation at Gebel Matulla.
Assemblage: Toward the late Maastrichtian, globotruncanids decreased and high abundances of biserial heterohelicids, pseudoguembelinids and triserial rugoglobigerinids are recorded (Fig. 7). The most characteristic assemblage recorded in this zone includes *Abathomphalus mayaroensis*, *Pseudoguembelina hariaensis*, *Rugoglobigerina scotti*, *Racemiguembelina fructicosa*, *Heterohelix globulosa*, *H. navaroensis*, *H. reussi*, *H. striata* and *Pseudotextularia elegans* (Fig. 7).
Remarks: The rarity of *Pseudoguembelina hariaensis* and *Racemiguembelina fructicosa*, which was also observed at the type locality of this zone in Tunisia (Nederbragt, 1990; Li and Keller, 1998a,b, Abramovich and Keller, 2002), makes correlation complex.. Therefore, lumping of the *Racemiguembelina fructicosa* (CF4) *Pseudoguembelina hariaensis* (CF3) and *Pseudoguembelina palpebra* (CF2) zones within the *Abathomphalus mayaroensis* Zone (CF4-CF2) may be more appropriate (Li et al., 1999). The use of the *Abathomphalus mayaroensis* Zone (CF4–CF2) for the late Maastrichtian below CF1 is more useful because of the rarity of *P. hariaensis* and *Racemiguembelina fructicosa*, which was also observed at the type locality of this zone in Tunisia (Nederbragt, 1990; Li and Keller, 1998b, Abramovich and Keller, 2002). The early–late Maastrichtian boundary is placed at the LO of *Racemiguembelina fructicosa* at 68.3 Ma (Li

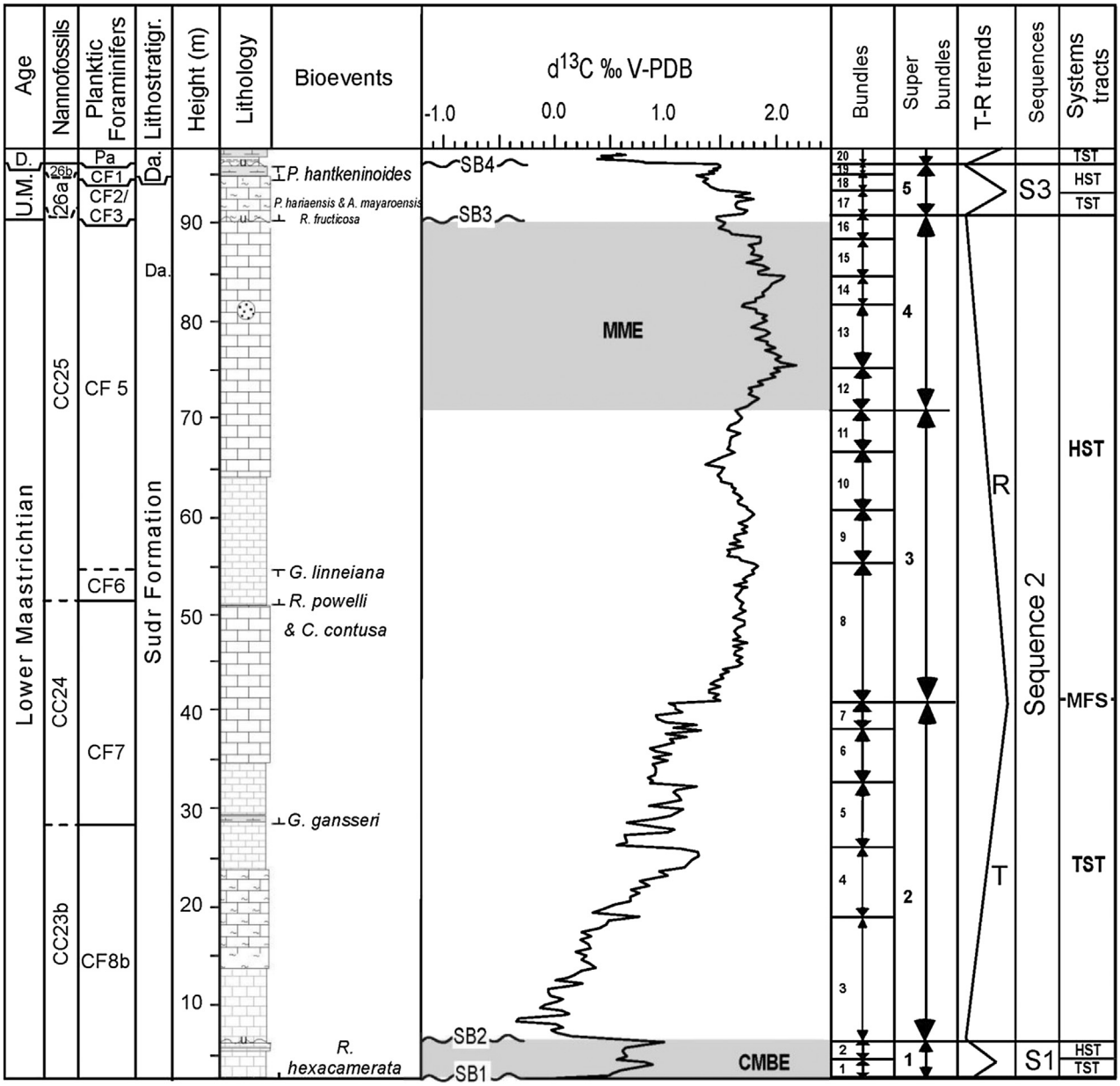

Fig. 9. Carbon isotope stratigraphy of the Matulla section and corresponding cyclic organization of the carbonate sediments. TST: Transgressive system tract; HST: Highstand system tract; MFS: maximum flooding surface; SB: sequence boundary.

et al., 1999). In the present study, the LO of *R. fructicosa* coincides with the LO of *Abathomphalus mayaroensis* Bolli and *Pseudoguembelina hariaensis* Nederbragt, and may denote the absence of Zone CF4 (Figs. 7 and 8).

4.6. Plummerita hantkeninoides *Zone (*CF1*)*

Definition: This zone is defined by the total range of the nominate species.
Author: It was first defined from Egypt by Masters (1984).
Thickness: Zone CF1 spans 1.5 m (samples 298 to 310) in the lowermost part of the Dakhla Formation.
Estimated age: latest Maastrichtian (65.3–65.0 Ma; Li et al., 1999).
Assemblage: The assemblage of this interval is similar to that of the underlying CF2 Zone with the addition of *Rugoglobigerina reicheli* (see Fig. 7 for the complete assemblage).

Remarks: This zone is approximately equivalent to the uppermost part of the *Abathomphalus mayaroensis* Zone of Caron (1985) and to the entire *Plummerita reicheli* Zone of Robaszynski et al. (2000), and represents the youngest Maastrichtian planktonic foraminiferal zone. The assemblage of this zone is similar to that of the underlying CF2 Zone with the addition of *Rugoglobigerina reicheli* Brönnimann (see Fig. 3 for the complete assemblage). *Plummerita hantkeninoides* is a warm-water species that appeared during the last 300 kyr of the Maastrichtian, close to the magnetochron boundary 30n/29r as estimated from the palaeomagnetic record at Agost, Spain (Pardo et al., 1996). Variable patterns in the thickness of Zone CF1 from 1.8 m to 8 m are associated with reworking of Maastrichtian foraminifera into lower Danian sediments around the K/Pg boundary. This reworking at the K/Pg boundary was observed in many parts of the world (Hendriks et al., 1987; Abramovich et al., 1998; Abramovich and Keller, 2002; Luciani, 2002; Keller, 2002; Farouk and Faris, 2008; Faris and Farouk, 2012).

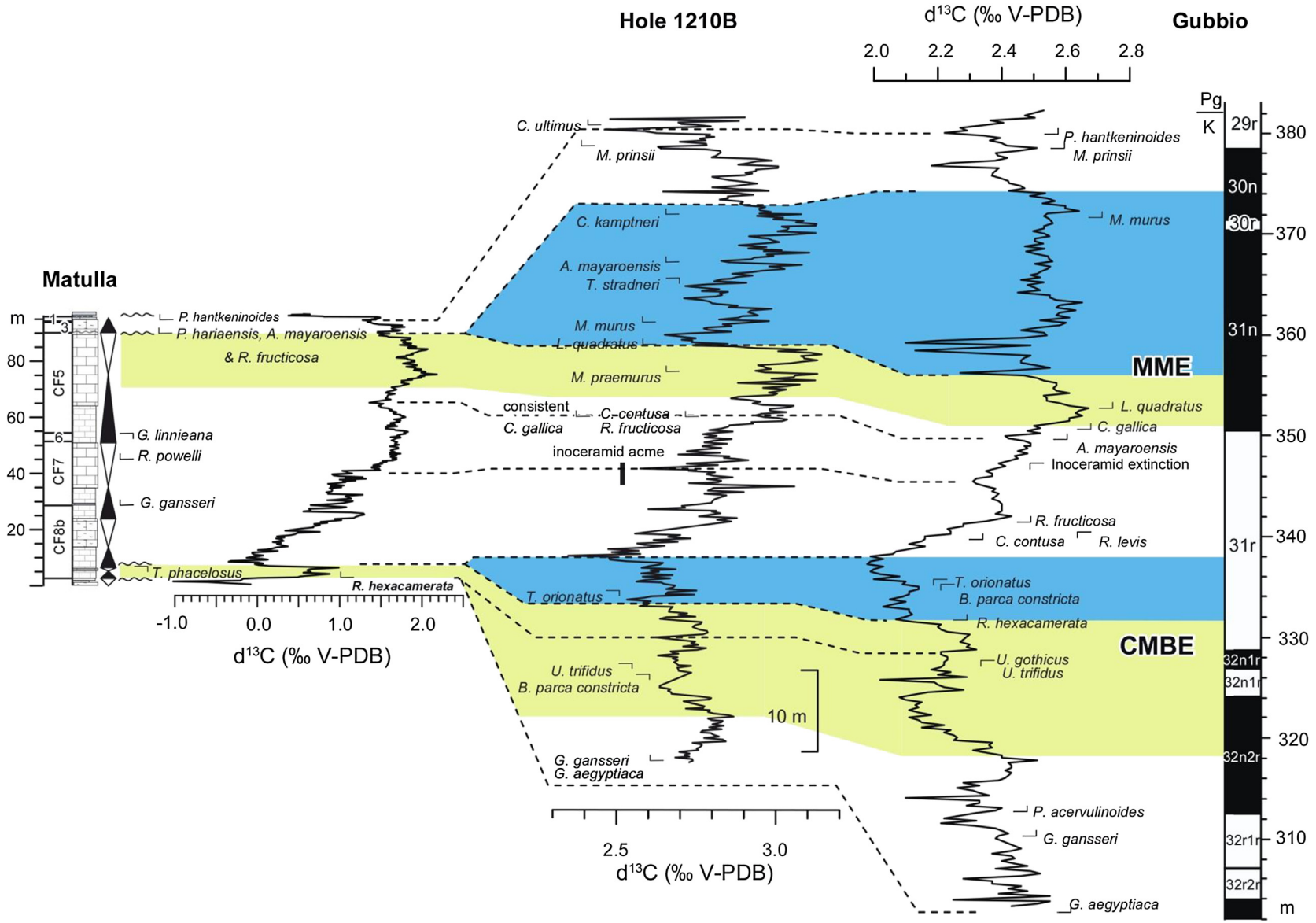

Fig. 10. Carbon isotope correlation of the Matulla section with the $\delta^{13}C$ records of Hole 1210B in the tropical Pacific and Gubbio, Italy (data from Voigt et al., 2012). Abbreviations of the nannofossil genera: *B.* = *Broinsonia*; *C.* = *Cribrocorona*; *L.* = *Lithraphidites*; *M.* = *Micula*; *R.* = *Reinhardtites*; *T.* = *Tranolithus*; *U.* = *Uniplanarius*.

5. $\delta^{13}C$ and Global correlation

The carbon-isotope record of the Matulla section shows pronounced variability on long- and short-term time scales, with values ranging from 0.02‰ to +2.18‰ (Fig. 9). The Matulla curve starts with small-scale positive excursions correlated with the base of Chron C31r of earliest Maastrichtian age, with values around 0.02‰ to 0.99‰ in the interval from 0.5 to 6.5 m (bundles 1 to 2; Fig. 9) related to the terminal Campanian–Maastrichtian Boundary Event (CMBE). This event is well known from stable isotope datasets from Tethys, deep sea and boreal chalk successions and is represented by a prominent negative carbon-isotope excursion that lasted around 2.5 Ma (Jarvis et al., 2002; Voigt et al., 2010; Jung et al., 2012; Voigt et al., 2012; Thibault et al., 2012a,b), with five small-scale positive excursions that encompass mid-Chron C32n2n to mid-Chron C31r (CMBE1-CMBE5; Voigt et al., 2012; Fig. 10). The termination of the CMBE, equivalent to CMBE5, falls into the gap identified in the Matulla section (Figs 9 and 10). The inferred hiatus correlates with the second hiatus dated between 69.9 and 69.0 Ma, in ODP Hole 1210B, recorded by Jung et al. (2012).

Correlation with the results from the Tercis les Bains GSSP and Gubbio sections suggests that the only part of the CMBE preserved is equivalent to CMBE4. The lowest occurrence of *Rugoglobigerina hexacamerata* was also identified in the lower parts of the Sudr Formation. The LO *Rugoglobigerina hexacamerata* event, as proposed by Li et al. (1999, 2000), defines the base of the Maastrichtian in the Tethyan Province. In the Gubbio, Contessa Highway and Bottaccione sections, as well as in the Tercis GSSP section, this event falls in the lower portion of Chronozone C31r (Voigt et al., 2012; Gardin et al., 2012). Therefore, it can be considered a reliable bioevent for the base of the Maastrichtian, since the zonal marker is easily and clearly recognizable and shows a sharp increase in abundance (Fig. 10).

The LO of *Rugoglobigerina scotti* (Brönnimann) is a primary stratigraphic datum marking the Campanian–Maastrichtian boundary in the Tercis GSSP section, but it is not applicable to the Matulla section because its LO is reported too high in the section, within Zone CF5 (Fig. 10).

Above the CMBE, the Matulla $\delta^{13}C$ curve is characterized by negative values in the interval from 8.6 to 40.8 m (−0.35‰ to 1.03‰ in superbundle 2, Fig. 9). Positive values start from the middle part of Zone CF7 and continue into the top part of Zone CF5, in the interval from 41 to 91 m, ranging from1.7‰ to a maximum 2.18‰ (bundles 8 to 16) and relate to a positive excursion within the mid-Maastrichtian Event (MME). The MME comprises a lower and an upper maximum, with a negative inflection in between at Hemmoor (Germany), Stevns-1 well (Danish Basin), Gubbio and Site 1210B (MME Peaks 1–3; Fig. 9, Voigt et al., 2012). The Matulla curve includes the lower maximum peak and lower negative inflection, while the termination of the MME falls into the identified hiatus at the Lower/Upper Maastrichtian contact, which supports the absence of the CF4 Zone (Figs. 9 and 10).

The interval above the MME and the identified gap is characterized by another short-term maximum, with values ranging from 1.28‰ to 1.79‰ (bundle 17). This part is followed by a long-term lower $\delta^{13}C$ minimum with values ranging from 1.79‰ to 1.28‰ (bundles 18 to 19), which starts in the middle of Zone CF2 and ends at the K/Pg boundary (Figs. 9 and 10). In the Matulla curve, the K/Pg boundary falls within another hiatus and only the lower $\delta^{13}C$ minimum of KPg-1 is preserved where the CF1 and P0 zones are missing (Figs. 9 and 10). A similar hiatus was recorded from ODP Hole 1210B (Jung et al., 2012; Voigt et al., 2012). In the interval from 96.1 to 97 m above the K/Pg boundary (Zone Pa), a typical negative excursion in the carbon isotope record is expressed in Gebel Matulla by a progressive decrease from 1.46‰ to a minimum 0.38‰. Similar trends were recorded above 12.8 m of the K/Pg boundary in the Stevns-1 well, Danish Basin (Thibault et al., 2012a).

6. Long-term depositional sequences

Within the ~100 m-thick intervals studied, portions of three longer-term transgressive-regressive depositional sequences were recognized in Sequences A, B and C (Fig. 9). Cyclical changes of foraminiferal assemblages (e.g. type, diversity/ abundance, and planktonic/benthic ratio) can be useful tools to detect transgressive-regressive trends, especially in the monotonous hemipelagic facies which is characterized by lacking physical boundaries and lithofacies changes.

6.1. Sequence A

Sequence A falls within the *Rugoglobigerina hexacamerata* planktonic foraminiferal Zone. It is bounded at the base by the Santonian/Maastrichtian sequence boundary (SB1) that unconformably separates the Matulla and Sudr formations, where the Campanian sediments are missing in the Gebel Matulla section, reflecting structural uplift which began in the latest Santonian and ended in the late Campanian (Guiraud and Bosworth, 1999; Guiraud et al., 2005; Figs. 3 & 4). SB1, across the Matulla and Sudr formational boundary, has been recorded by various authors in Sinai (e.g. Lüning et al., 1998; El-Sheikh, 1999; Obaidalla and Kassab, 2002; El-Azabi and El-Araby, 2007; and Farouk and Faris, 2012), based on obvious facies and palaeontological changes. The underlying uppermost portion of the Matulla Formation is barren of foraminifera and most likely denotes the effect of the major fall in eustatic sea level that characterized the end of the Santonian (Haq et al., 1987; Hardenbol et al., 1998). However, this boundary is easily recognized in the field by the sharp contact of the mixed siliciclastic/carbonate Matulla Formation and the overlying transgressive carbonate facies of the Sudr Formation (Figs. 3 and 4). The basal part of sequence A is interpreted as a retrogradational parasequence (bundle 1) characterized by stacked foraminiferal carbonates, marking a rise in relative sea level that resulted in the deposition of middle neritic hemipelagic chalk (Fig. 9). These hemipelagic facies are characterized by variable abundances of foraminifera; the open marine conditions probably resulted in a low sedimentation rate. Benthic foraminiferal assemblage (F) of a Midway-Fauna Type (Berggren and Aubert, 1975) indicates a transgressive system tract. A few agglutinated genera (4–6%), represented by *Spiroplectammina* and *Gaudryina*, reflect deposition above the carbonate compensation depth in an environment that was rich in calcium carbonate, well oxygenated and of normal salinity (Table 1). This was followed by a regressive cycle which was characterized by large amounts of beach sand and iron-rich clasts with decreased percentages of planktonic foraminifera (53.7–20.2) and a low percentage of deep-water keeled planktonic morphotypes. This regressive cycle shows a corresponding increase in rugoglobigerinids and Heterohelicidae, with a *Cibicides*-dominated benthic assemblage, denoted by a highstand systems tract comprising a shallow, inner-neritic carbonate mudstone parasequence (bundle 2). The top of depositional sequence A is characterized by another sequence boundary (SB2), marked by the absence of the terminal Campanian–Maastrichtian Boundary Event (CMBE). This event is known from stable isotope datasets around the world (Jung et al., 2012) and is coincident with a major global cooling event and eustatic sea-level fall which occurred at 71 Ma (Haq et al., 1987; Hardenbol et al., 1998; Li and Keller, 1998a).

Table 1
Summary of the sequence stratigraphic interpretation of the depositional sequences inferred in Gebel Matulla, showing their stratigraphic levels, P/(P + B)%, the diversity as well as the dominant benthic foraminiferal assemblages.

Planktonic biozones	P/B ratio	Diversity	Characteristic benthic assemblages	Assemblages	Sedimentary environments	System tract tracts
CF1–upper CF2	30–40%	Medium	*Bolivina incrassata gigantea*, *Bulimina reussi*, *Lenticulina pseudosecans*, *Dentalina granti* and *Pseudoclavulina asper whitei*	A	Middle neritic	HST
CF3–lower CF2	75–60%	High	*Cibicidoides succedens*, *C. pseudoacutus*, *C. hyphalus*, *Alabamina midwayensis*, *Angulogavelinella avnimelechi.*	B	Outer neritic	TST
CF5–upper CF7	20.2–53.7%	Very low	*Coryphostoma incrassata*, *Gavelinella limbata*, *Nonionella cretacea*, *N. robusta*, *Osangularia expansa*,	C	Inner neritic	HST
Lower CF7–CF8b	20.2–73.7%)	Very high	*Bolivinoides draco draco*, *B. draco miliaris*, *Gaudryina pyramidata*, *Bolivina incrassata incrassata*	**D**	Outer neritic	TST
CF8b	20.2–53.7%	Medium	*Cibicides tappanae*, *C. praecursorius*, *Gavelinella limbata*, *G. paleocenica*, *Gyroidinoides globosus*, *Bolivina incrassata incrassata.*	E	Inner neritic	HST
	53.7%	High	*Lenticulina obesus*, *L. midwayensis*, *Anomalinoides grandis*, *A. sinaensis*, *Spiroplectammina knebeli*, *Gaudryina pyramidata*, *Tritaxia baraki*	F	Middle neirtic	TST

6.2. Sequence B

This depositional sequence comprises most of the Sudr Formation and falls within planktonic foraminiferal zones CF7 through CF5. A transgressive systems tract (superbundle 2) marks a rise in relative sea level that resulted in the deposition of outer neritic hemipelagic chalk (Fig. 9). These hemipelagic facies are characterized by an increase in the percentages of planktonic foraminifera (20.2–73.7%), resulting in the maximum diversity of globotruncanids and the deeper marine benthic foraminifer genus *Bolivinoides*, which suggest open ocean conditions (Table 1). A similar trend was observed in the Tethys and South Atlantic (Li and Keller, 1988a,b) in Maastrichtian deposits. The overlying progradational highstand facies (superbundle 3 and 4) is indicated by a decrease in the planktonic percentages (73.7–20.7%). This is associated with a decrease in globotruncanids and deep benthic foraminiferal assemblages. The Lower/Upper Maastrichtian boundary is not easily recognized in the field, due to the lack of a physical boundary and the monotonous carbonate hemipelagic facies. The L/U Maastrichtian hiatus records the missing CF4 Zone and separates the upper regressive cycle occurring within the CF5 Zone from the overlying Upper Maastrichtian transgressive cycle occurring within the CF6 Zone. This event corresponds to the well-defined Mid-Maastrichtian event (MME) in the Gubbio curve (Voigt et al., 2012) and the previously identified gap in the Indian Ocean (ODP Hole 762C; Thibault et al., 2012b).

6.3. Sequence C

Sequence C comprises the uppermost part of the Sudr Formation and occurs within planktonic foraminiferal zones CF3 through CF1. It is reduced in thickness from 90.6 to 96 m (superbundle 5; Fig. 9). The transgressive systems tract (TST) consists of bundle 17 and is characterized by high planktonic/benthic ratios, with high diversity benthic foraminiferal assemblages (B) indicating an outer neritic environment for this interval. The MFS coincides with the maximum abundance of planktonic foraminifera and marks the change from deepening-upward to shallowing-upward biofacies deposits. The overlying regressive deposits (HST; bundles 18 & 19) exhibit a clear drop in the planktonic/benthic (P/B) ratio. The increase in heterohelicids and non-keeled planktonic forms, combined with a very low abundance of globotruncanids (<1%) in the upper part of Zones CF2 and CF1, and benthic assemblages (A), reflect a decline in sea level (Table 1). A relative sea-level drop is recorded during the latest Maastrichtian in the global eustatic cycle charts of Haq et al. (1987). At the Gebel Matulla section, the K/Pg boundary is characterized as missing the top part of the K/Pg event, the extinction of Cretaceous tropical planktonic foraminifera and an abrupt change in species richness, as recorded in several parts of Egypt. The K/Pg hiatus is recorded in several parts of Egypt, Tunisia, Libya, Negev and Jordan, as well as in several parts of the Arabian Shelf (Faris and Farouk, 2012; Luciani, 2002; Adatte et al., 2005; Alsharhan and Narin, 1995). However, the duration of this hiatus is variable, resulting from a variation in regional deposition and erosion, depending upon location. This hiatus may be linked to tectonic activity and irregular palaeotopography associated with low sedimentation rates as suggested by Farouk and Faris (2008).

7. Conclusions

A new planktonic foraminiferal biostratigraphy and calibrated $\delta^{13}C$ record from the Matulla section can be correlated to global Maastrichtian carbon cycle changes and global eustatic charts.

Comparison of the Maastrichtian planktonic foraminifera bio-events from the southern Tethyan margin with the Tercis les Bains GSSP, and Gubbio section and with ODP Hole 1210B revealed variations in the stratigraphic range of most Maastrichtian planktonic foraminiferal marker species. Most of these planktonic foraminiferal bio-events relate to globotruncanids and other keeled planktonic forms which show cold-water affinities and therefore appear early at mid-high latitudes, rather than in the warm waters of the Tethyan Province (Apthorpe, 1979; Braalower and Siesser, 1992; Wonders, 1992; Shafik, 1998; Petrizzo, 2000; Howe et al., 2003; Thibault et al., 2012a,b; Farouk and Faris, 2012).

The LO of *Rugoglobigerina hexacamerata* is a useful datum for the identification of the base of the Maastrichtian Stage, since the defining criterion proposed at the Tercis les Bains GSSP section (LOs of *Contusotruncana contusa* and *Rugoglobigerina scotti*) are reported as too high in the present study and does not seem to be applicable in the southern Tethyan Province.

The sedimentary succession of the Maastrichtian Sudr Formation comprises basinal chalks and platform limestones which allow the identification of significant negative excursions within Maastrichtian $\delta^{13}C$ events, namely the Campanian–Maastrichtian Boundary Event (CMBE), the mid-Maastrichtian Event (MME), and the Cretaceous–Palaeogene Event (KPgE). Termination of these well known $\delta^{13}C$ events are associated with four unconformities which cover (1) the upper Santonian to upper Campanian; (2) the late CMBE; (3) the uppermost MME and large parts of the Upper Maastrichtian; and (4) the K/Pg boundary interval.

Correlation with the global eustatic charts (Haq et al., 1987; Hardenbol et al., 1998; Li et al., 2000; Miller et al., 2005) shows a clear similarity, indicating that eustasy was the main control and a pulse of tectonic uplift affected the duration of these hiatus, which are characterized by lacking the significant terminal negative excursion of the Maastrichtian $\delta^{13}C$ events.

Acknowledgements

Gratitude is expressed to Silke Voigt (Goethe-University of Frankfurt) for measuring the stable isotopes, helpful comments, and suggestions. Many thanks also to Haydon W. Bailey (Potters Bar, UK) for reviewing the manuscript; and to A.J. Tafoya (University of New Mexico) for reading an early version of the manuscript, as well as to C.J. Wood (Minehead, UK) for editorial work and giving me many helpful suggestions.

References

Abed, A.M., Ashour, N., 1987. Petrography and age determination of the NW Jordan phosphorites. Dirasat 14, 247–263.
Abramovich, S., Almogi-Labin, A., Bejamini, C., 1998. Decline of the Maastrichtian pelagic ecosystem based on planktic foraminiferal assemblage change: implications for terminal Cretaceous faunal crisis. Geology 26, 63–66.
Abramovich, S., Keller, G., 2002. High stress late Maastrichtian paleoenvironment: Inferences from planktic foraminifera in Tunisia. Palaeogeography. Palaeoclimatology Palaeoecology 178, 145–164.
Adatte, T., Keller, G., Stüben, D., Harting, M., Kramar, U., Stinnesbeck, W., Abramovich, S., Benjamini, C., 2005. Late Maastrichtian and K/T paleoenvironment of the eastern Tethys (Israel): mineralogy, trace and platinum group elements, biostratigraphy and faunal turnovers. Bulletin de la Société Géologique de France 176 (no 1), 37–55.
Alsharhan, A.S., Narin, A.E.M., 1995. Tertiary of the Arabian Gulf: sedimentology and hydrocarbon potential. Palaeogeography, Palaeoclimatology, Palaeoecology 114, 369–384.
Al-Wosabi, K., Abu Shama, A.Z., 2007. Planktonic foraminiferal and calcareous nannofossil biostratigraphy around the K/P boundary at Matulla section, west central Sinai. Egyptian Journal of Paleontology 7, 87–115.
Apthorpe, M.C., 1979. Depositional history of the Upper Cretaceous of the Northwest shelf, based upon Foraminifera. The APPEA Journal 19, 74–89.
Ayyad, S.N., Faris, M., El Nahass, H.A., Saad, K.A.A., 2003. Planktonic foraminiferal and calcareous nannofossil biostratigraphy from the Upper Cretaceous-Lower Eocene successions in northeast Sinai, Egypt, 3rd International Conference on the Geology of Africa, Assiut 1, pp. 649–683.
Barrera, E., Huber, B.T., 1990. Evolution of Antarctic waters during the Maestrichtian: Foraminifer oxygen and carbon isotope ratios, Leg 113. In: Barker, P.F., Kennett, J.P., et al. (Eds.), Proceedings of the Ocean drilling program, Scientific Results, 113, pp. 813–827.
Barrera, E., Savin, S.M., 1999. Evolution of late Campanian-Maastrichtian marine climates and oceans. In: Barrera, E.J., Johnson, C.C. (Eds.), Evolution of the Cretaceous Ocean-Climate System, Geological Society of America Special Paper, 332, pp. 245–282.
Berggren, W.A., Aubert, J., 1975. Paleocene benthonic foraminiferal biostratigraphy, paleobiogeography and paleoecology of Atlantic-Tethyan regions: Midway-type fauna. Palaeogeography, Palaeoclimatology, Palaeoecology 18, 73–192.
Braalower, T.J., Siesser, W., 1992. Cretaceous calcareous nannofossil biostratigraphy of Sites 761, 762 and 763, Exmouth and Wombat Plateaus, northwest Australia. Proceedings of the Ocean Drilling Program, Scientific Results 122, 529–556.
Burnett, J.A., with contributions from Gallagher, L.T., Hampton, M.J., 1998. Upper Cretaceous. In: Bown, P.R. (Ed.), Calcareous Nannofossil Biostratigraphy. British Micropalaeontological Society Publications Series. Chapman and Hall/ Kluwer Academic Publishers, London, 132–199.
Caron, M., 1985. Cretaceous planktic foraminifera. In: Bolli, H.M., Saunders, J.B., Perch-Nielsen, K. (Eds.), Plankton Stratigraphy. Cambridge University Press, Cambridge, pp. 17–86.
Crampton, J.S., Schiøler, P., Roncaglia, L., 2006. Detection of Late Cretaceous eustatic signatures using quantitative biostratigraphy. Geological Society of America Bulletin 118, 975–990.
El-Azabi, M.H., El-Araby, A., 2007. Depositional framework and sequence stratigraphic aspects of the Coniacian–Santonian mixed siliciclastic/carbonate Matulla sediments in Nezzazat and Ekma blocks, Gulf of Suez, Egypt. Journal of African Earth Sciences 47, 179–202.
El-Azabi, M.H., Farouk, S., 2011. High-resolution sequence stratigraphy of the Maastrichtian-Ypresian succession along the eastern scarp face of the Kharga Oasis, south Western Desert, Egypt. Sedimentology 58, 579–617.
El-Sheikh, H.A., 1999. Coniacian–Late Campanian boundaries in Sinai, 1st conference on the Geology of Africa, Assiut, Egypt, pp. 5–20.
Faris, M., Farouk, S., 2012. Integrated biostratigraphy of the Upper Maastrichtian – Paleocene successions in north-central Sinai, Egypt. Geologia Croatica 65/2, 139–160.
Faris, M., Abu Shama, A.M., 2006. Calcareous nannofossils of the Campanian-Maastrichtian Sudr Formation in Abu Zenima area, West Central Sinai. Egyptian Journal of Paleontology 6, 251–274.
Farouk, S., Faris, M., 2008. Campanian to Eocene planktic foraminiferal and calcareous nannofossil biostratigraphy in the synclinal areas around Gebel Libni, North Sinai, Egypt. Middle East Research Center Ain Shams University, Earth Science Series 22, 187–201.
Farouk, S., Faris, M., 2012. Late Cretaceous calcareous nannofossil and planktonic foraminiferal bioevents of the shallow-marine carbonate platform in the Mitla Pass, west central Sinai, Egypt. Cretaceous Research 33, 50–65.
Friedrich, O., Herrle, J.O., Wilson, P.A., Cooper, M.J., Erbacher, J., Hemleben, C., 2009. Early Maastrichtian carbon cycle perturbation and cooling event: implications from the South Atlantic Ocean. Paleoceanography 24, PA2211. http://dx.doi.org/10.1029/2008PA001654.
Gardin, S., Galbrun, B., Thibault, N., Coccioni, R., Premoli Silva, I., 2012. Bio-magnetochronology for the upper Campanian-Maastrichtian from the Gubbio area, Italy: new results from the Contessa Highway and Bottaccione sections. Newsletters on Stratigraphy 45/1, 75–103.
Ghorab, M.A., 1961. Abnormal stratigraphic features in Ras Gharib oil field. In: 3rd Arab Petroleum Congress, Alexandria, Egypt, 10 pp.
Guiraud, R., Bosworth, W., 1999. Phanerozoic geodynamic evolution of northeastern Africa and the northwestern Arabian platform. Tectonophysics 315, 73–108.
Guiraud, R., Bosworth, W., Thierry, J., Delplanque, A., 2005. Phanerozoic geological evolution of Northern and Central Africa: An overview. Journal of African Earth Sciences 43, 83–143.
Haq, B.U., Hardenbol, J., Vail, P.R., 1987. Mesozoic and Cenozoic chronostratigraphy and cycles of sea-level change. SEPM Special Publication 42, 71–108.
Hardenbol, J., Thierry, J., Farley, M.B., Jacquin, T., de Graciansky, P.-C., Vail, P.R., 1998. Mesozoic-Cenozoic sequence chronostratigraphy framework of European basins. In: de Graciansky, P.-C., Hardenbol, J., Jacquin, T., Vail, P.R. (Eds.), Sequence stratigraphy of European basins, SEPM Special Publication, 60, pp. 3–14.
Hendriks, F., Luger, P., Bowitz, J., Kallenbach, H., 1987. Evolution of the depositional environments of the SE-Egypt during the Cretaceous and Lower Tertiary. Berliner Geowissenschaftliche Abhandlungen A 75, 49–82. Berlin.
Hewaidy, A.A., El-Azabi, M.H., Farouk, S., 2006. Facies associations and sequence stratigraphy of the Upper Cretaceous-Lower Eocene succession in the Farafra Oasis, Western Desert, Egypt, 8th International Conference of Arab world, Cairo University II, pp. 569–599.
Howe, R.W., Campbell, R.J., Rexilius, J.P., 2003. Integrated uppermost Campanian–Maastrichtian calcareous nannofossil and foraminiferal biostratigraphic zonation of the northwestern margin of Australia. Journal of Micropalaeontology 22, 29–62.
Huber, B.T., 1992. Paleobiogeography of Campanian–Maastrichtian foraminifera in the southern high latitudes. Palaeogeography, Palaeoclimatology. Palaeoecology 92, 325–360.
Huber, B.T., Watkins, D.K., 1992. Biogeography of Campanian–Maastrichtian calcareous plankton in the region of the Southern Ocean: Paleogeographic and Paleoclimatic implications. In: Kennett, J.P., Warnke, D.A. (Eds.), The Antarctic Paleoenvironment: A Perspective on Global Change: American Geophysical Union, Antarctic Research Series 56American Geophysical Union, Washington, pp. 31–60.
Jarvis, I., Mabrouk, A., Moody, R.T.J., de Cabrera, S., 2002. Late Cretaceous (Campanian) carbon isotope events, sea level change and correlation of the Tethys and Boreal realms. Palaeogeography, Palaeoclimatology, Palaeoecology 188, 215–248.
Jung, C., Voigt, S., Friedrich, O., 2012. High-resolution carbon-isotope stratigraphy across the Campanian-Maastrichtian boundary at Shatsky Rise (tropical Pacific). Cretaceous Research 37, 177–185.
Keller, G., 2002. Guembelitria-dominated late Maastrichtian planktic foraminiferal assemblages mimic early Danian in central Egypt. Marine Micropaleontology 47, 71–99.
Lees, J.A., 2002. Calcareous nannofossil biogeography illustrates palaeoclimate change in the Late Cretaceous Indian Ocean. Cretaceous Research 23, 537–634.
Li, L., Keller, G., 1998a. Maastrichtian climate, productivity and faunal turnovers in planktic foraminifera in South Atlantic DSDP Sites 525 and 21. Marine Micropaleontology 33, 55–86.
Li, L., Keller, G., 1998b. Diversification and extinction in Campanian-Maastrichtian planktic foraminifera of northwest Tunisia. Eclogae Geologica Helvetica 91, 75–102.
Li, L., Keller, G., Stinnesbeck, W., 1999. The Late Campanian and Maastrichtian in northwestern Tunisia: paleoenvironmental inferences from lithology, macrofauna and benthic foraminifera. Cretaceous Research 20, 231–252.
Li, L., Keller, G., Adatte, T., Stinnesbeck, W., 2000. Late Cretaceous sea-level changes in Tunisia: a multi-disciplinary approach. In: Special Publication, 157. Geological Society, London, pp. 447–458.
Luciani, V., 2002. High-resolution planktonic foraminiferal analysis from the Cretaceous-Tertiary boundary at Ain Settara (Tunisia): evidence of an extended mass extinction. Paleogeography, Palaeoclimatology, Palaeoecology 178, 299–329.
Luger, P., 1988. Maastrichtian to Paleocene facies evolution and Cretaceous/Tertiary boundary in middle and southern Egypt. Revista Espanola de Paleontologia, Numero extraordinario, 83–90.

Lüning, S., Marzouk, A., Kuss, J., 1998. The Paleocene of central east Sinai, Egypt: 'sequence stratigraphy' in monotonous hemipelagites. Journal of Foraminiferal Research 28, 19–39.
Masters, B.A., 1984. Comparison of planktonic foraminifers at the Cretaceous-Tertiary boundary from the El Haria shale (Tunisia) and the Esna shale (Egypt). Proceedings of the 7th Exploration Seminar, March, 1984, Cairo, Egypt. Egyptian General Petroleum Corporation, pp. 310–324.
Miller, K.G., Kominz, M.A., Browning, J.V., Wright, J.D., Mountain, G.S., Katz, M.E., Sugarman, P.J., Cramer, B.S., Christie-Blick, N., Pekar, S.F., 2005. The Phanerozoic record of global sea-level change. Science 312, 1293–1298.
Nederbragt, A.J., 1990. Biostratigraphy and paleoceanographic potential of the Cretaceous planktic foraminifera Heterohelicidae [Ph.D. thesis]. Centrale Huisdrukkerij Vrije Universiteit, Amsterdam, 203 pp.
Obaidalla, N.A., Kassab, A.S., 2002. Integrated biostratigraphy of the Coniacian-Santonian sequence, southwestern Sinai, Egypt. Egyptian Journal of Paleontology 2, 85–104.
Odin, G.S. (Ed.), 2001. The Campanian–Maastrichtian Stage Boundary – characterization at Tercis les Bains (France) and correlation with Europe and other continents. Developments in Paleontology and Stratigraphy, 19, 881 pp.
Osman, A., 2003. Late Campanian-Maastrichtian foraminifera from the Simsima Formation on the western side of the Northern Oman Mountains. Cretaceous Research 24, 391–405.
Pardo, A., Ortiz, N., Keller, G., 1996. Latest Maastrichtian and K/T boundary foraminiferal turnover and environmental changes at Agost, Spain. In: Macleod, N., Keller, G. (Eds.), Cretaceous-Tertiary mass extinction: biotic and environmental changes. Norton Press, pp. 139–171.
Pérez-Rodríguez, I., Lees, J.A., Larrasoaña, J.C., Arz, J.A., Ignacio Arenillas, I., 2012. Planktonic foraminiferal and calcareous nannofossil biostratigraphy and magnetostratigraphy of the uppermost Campanian and Maastrichtian at Zumaia, northern Spain. Cretaceous Research 37, 100–126.
Petrizzo, M.R., 2000. Upper Turonian-lower Campanian planktonic foraminifera from southern mid-high latitudes (Exmouth Plateau, NW Australia): biostratigraphy and taxonomic notes. Cretaceous Research 21, 479–505.
Premoli Silva, I., Sliter, W.V., 1995. Cretaceous planktonic foraminiferal biostratigraphy and evolutionary trends from the Bottaccione section, Gubbio, Italy. Paleontographia Italica 82, 1–89.
Robaszynski, F., Caron, M., 1995. Foraminifères planctoniques du Crétacé: commentaire de la zonation Europe–Méditerranée. Bulletin de la Société Géologique de France 166, 681–692.
Robaszynski, F., González-Donoso, J.M., Linares, D., Amédro, F., Caron, M., Dupuis, C., Dhondt, A.V., Gartner, S., 2000. Le Crétacé Supérieur de la région de Kalaat Senan, Tunisie centrale. Litho-Biostratigraphy intégrée: zones d'ammonites, de foraminifères planctoniques et de nannofossiles du Turonien supérieur au Maastrichtien. Bulletin du Centre de Recherches. Exploration-Production Elf Aquitaine 22, 359–490.
Samir, A., 2002. Biostratigraphy and paleoenvironment changes in the Upper Cretaceous-Early Paleogene deposits of Gabal Samra section, southwestern Sinai. Egyptian Journal of Paleontology, 1–40.
Shafik, S., 1990. Late Cretaceous nannofossil biostratigraphy and biogeography of the Australian western margin. Bureau of Mineral Resources, Geology and Geophysics Report 295, 1–164.
Shafik, S., 1998. Problems with the Cretaceous biostratigraphic system of Australia: time for a review. Australian Geological Survey Organisation Research Newsletter 28, 12–14.
Simmons, M.D., Sharland, P.R., Casey, D.M., Davies, R.B., Sutcliffe, O.E., 2007. Arabian plate sequence stratigraphy: Potential implications for global chrono-stratigraphy. GeoArabia 12, 101–130.
Speijer, R.P., Van der Zwaan, G.J., 1996. Extinction and survivorship in southern Tethyan benthic foraminifera across the Cretaceous/Paleogene boundary. In: Hart, M.B. (Ed.), Biotic Recovery from Mass Extinction Events, Geological Society Special Publication, 102, pp. 343–371.
Thibault, N., Gardin, S., 2010. The calcareous nannofossil response to the end-Cretaceous warm event in the Tropical Pacific. Palaeogeography, Palaeoclimatology, Palaeoecology 291, 239–252.
Thibault, N., Harlou, R., Schovsbo, N., Schiøler, P., Lauridsen, B.W., Sheldon, E., Stemmerik, L., Surlyk, F., 2012a. Upper Campanian-Maastrichtian nannofossil biostratigraphy and high-resolution carbon-isotope stratigraphy of the Danish Basin: Towards a standard d13C curve for the Boreal Realm. Cretaceous Research 33, 72–90.
Thibault, N., Husson, D., Harlou, R., Gardin, S., Galbrun, B., Huret, E., Minoletti, F., 2012b. Astronomical calibration of upper Campanian–Maastrichtian carbon isotope events and calcareous plankton biostratigraphy in the Indian Ocean (ODP Hole 762C): Implication for the age of the Campanian–Maastrichtian boundary. Palaeogeography, Palaeoclimatology, Palaeoecology 337–338, 52–71.
Voigt, S., Friedrich, O., Norris, R.D., Schönfeld, J., 2010. Campanian – Maastrichtian carbon isotope stratigraphy: shelf-ocean correlation between the european shelf and the tropical Pacific Ocean. Newsletters on Stratigraphy 44, 57–72.
Voigt, S., Gale, A., Jung, C., Jenkyns, H., 2012. Global correlation of Upper Campanian – Maastrichtian successions using carbon isotope stratigraphy: development of a new Maastrichtian timescale. Newsletters on Stratigraphy 45, 25–53.
Wonders, A.A.H., 1992. Cretaceous planktonic foraminiferal biostratigraphy, Leg 122, Exmouth Plateau, Australia. Proceedings of the Ocean Drilling Program. Scientific Results 122, 587–600.